Final state interaction effects in $D(e, e'p)$ scattering

A. Bianconi [a,b], S. Jeschonnek [c], N.N. Nikolaev [c,d], B.G. Zakharov [c,d]

[a] *Istituto Nazionale di Fisica Nucleare, Sezione di Pavia, Pavia, Italy*
[b] *Dipartimento Fisica Nucleare e Teorica, Università di Pavia, Italy*
[c] *IKP (Theorie), Forschungszentrum Jülich GmbH., D-52425 Jülich, Germany*
[d] *L.D. Landau Institute for Theoretical Physics, GSP-1, 117940, ul. Kosygina 2, V-334 Moscow, Russia*

Abstract

We present a systematic study of the final-state interaction (FSI) effects in $D(e,e'p)$ scattering in the CEBAF energy range with particular emphasis on the phenomenon of the angular anisotropy of the missing momentum distribution. We find that FSI effects dominate at missing momentum $p_m \gtrsim 1.5$ fm^{-1}. FSI effects in the excitation of the S-wave state are much stronger than in the excitation of the D-wave.

There is a basic necessity of the knowledge of the nucleon momentum distribution $n(p)$ in nuclei, in particular at large momenta, for it provides unique information on short-distance nucleon-nucleon interaction (initial-state N-N correlations ISC) in the nuclear medium ([1], for a recent review see [2]). A quantitative understanding of the final-state interaction (FSI) effects is crucial for disentangling $n(p)$ from the missing momentum distribution $W(p_m)$ as measured in inclusive $A(e,e'p)$ scattering in quasielastic kinematics. In a previous paper [3] on ^{4}He$(e,e'p)$ scattering we found that at large missing momenta p_m, which are usually believed to come from the ISC effects, the FSI effects are large and overwhelm the ISC effects (for the case of heavy nuclei see also [4–6]). In [3] the FSI was shown to produce a strong angular anisotropy of $W(p_m)$, which at large p_m develops a sharp peak in transverse kinematics, at $\theta \sim 90°$, two minor peaks at $\theta = 0°$ and $180°$ in parallel kinematics and a sizable backward-forward asymmetry (here θ is the angle between the missing momentum and the

(e, e') momentum transfer $\boldsymbol{q}$).

To generalize these results and get a deeper insight into them, in this paper a systematic study of the $D(e, e'p)n$ unpolarized scattering is performed. Prediction of FSI effects in this process is of great interest on its own sake, as experiments with the deuterium target constitute an important part of the experimental program at CEBAF [7]. Other motivations are that (i) in the region of dominance of ISC effects, the momentum distribution for heavy nuclei are expected to closely resemble that in the deuteron [8]; (ii) the realistic models of the deuteron [9] allow an accurate evaluation of FSI effects in the longitudinal missing momentum distribution which is important for the y-scaling analysis [10]; (iii) one can assess differences between FSI effects for the S and D waves in the initial N-N pair. Despite the deuteron being a dilute target, we find large FSI effects at $p_m \gtrsim 1.5$ fm^{-1}.

One of the points we wish to address in more detail are forward and backward peaks in $W(\boldsymbol{p}_m)$, which have their origin in the idealized step-function factor

$\theta(z)$ in the eikonal Green function derived [11] under an implicit assumption of pointlike nucleons (z is the longitudinal separation of nucleons). We analyze the sensitivity of the forward and backward peaks to the smearing of the θ-function to account for the finite size of nucleons and conclude that predictions at $p_m \lesssim 3$ fm^{-1} are free of uncertainties with the smearing.

We wish to focus on FSI effects, and for the sake of simplicity we consider the photon as a scalar operator (for the full hadronic tensor in deuteron scattering, see Ref. [12]). Then, the reduced nuclear amplitude for the exclusive process $D(e, e'p)n$ is given by $\mathcal{M}_{ji} = \int d^3 r \exp(i p_m r) \chi_j^* S(r) \Psi_i(r)$, where $r \equiv r_n - r_p$, $\Psi_i(r)$ is the deuteron wave function for the spin state i and χ_j stands for the spin wave function of the final pn state. The struck proton is detected with momentum P, q is the (e, e') momentum transfer and $p_m \equiv P - q$ is the missing momentum. $S(r)$ is the S-matrix of FSI between struck proton and spectator neutron. For unpolarized deuterons and for a spin-independent proton-neutron scattering amplitude, one finds the observed momentum distribution

$$W(\boldsymbol{p}_m) = \frac{1}{3} \sum_{j,i} |M_{ji}|^2 = \frac{1}{4\pi(2\pi)^3}$$

$$\times \int d^3 r d^3 r' \exp[i\boldsymbol{p}_m \cdot (\boldsymbol{r}' - \boldsymbol{r})] S(r) S^\dagger(r')$$

$$\times \left[\frac{u(r)}{r} \frac{u(r')}{r'} + \frac{1}{2} \frac{w(r)}{r} \frac{w(r')}{r'} \left(3 \frac{(\boldsymbol{r} \cdot \boldsymbol{r}')^2}{(rr')^2} - 1 \right) \right], \tag{1}$$

where u/r and w/r are the S and D-wave radial wave functions of the deuteron, with the normalization $\int dr(u^2 + w^2) = 1$. We have used the realistic Bonn wave functions [9].

At the large $Q^2 \gtrsim (1-2)$ GeV^2 of the interest in the CEBAF experiments, the kinetic energy of the struck proton $T_{\text{kin}} \approx Q^2/2m_p$ is high and FSI can be described by Glauber theory [11]. Defining transverse and longitudinal components $\boldsymbol{r} \equiv (\boldsymbol{b} + z\hat{q})$ we can write

$$S(\boldsymbol{r}) = 1 - \theta(z) \Gamma(\boldsymbol{b}), \tag{2}$$

where $\Gamma(\boldsymbol{b})$ is the profile function of the proton-neutron scattering, which at high energy can conveniently be parameterized as

$$\Gamma(\boldsymbol{b}) \equiv \frac{\sigma_{\text{tot}}(1 - i\rho)}{4\pi b_0^2} \exp\left[-\frac{b^2}{2b_0^2} \right] \tag{3}$$

(ρ is the ratio of the real to imaginary part of the forward elastic scattering amplitude). The step-function $\theta(z)$ in (2) tells that the FSI vanishes unless the spectator neutron was in the forward hemisphere with respect to the struck proton. A thorough test of the Glauber theory in the scattering of 2 GeV polarized deuterons on protons has been performed in [13], higher energy data on elastic pd scattering are discussed in [14], a generic review on the Glauber theory analysis of nucleon-nucleus scattering is given in [15]. Here we present numerical results for $T_{\text{kin}} \sim$ 1GeV ($Q^2 \sim 2$ GeV^2), when $b_0 \approx 0.5$ fm, $\sigma_{\text{tot}} \approx 40$ mb and $\rho \approx -0.4$ [15-17].

Let us start with generic observations on the symmetry properties of $W(\boldsymbol{p}_m)$. Decompose $\boldsymbol{p}_m$ into the transverse and longitudinal components $\boldsymbol{p}_m = \boldsymbol{p}_\perp + p_z\hat{q}$. In the plane-wave-impulse approximation (PWIA) $S(r) = 1$ and (1) gives the isotropic distribution $W(\boldsymbol{p}_m) = n(p_m)$. The radius b_0 of FSI is much smaller than the radius of the deuteron $R_D \sim 2$ fm. Consequently, as compared to $u(r), w(r)$, the FSI operator $\theta(z)\Gamma(\boldsymbol{b})$ is a "short-ranged" function of $\boldsymbol{b}$ and a "long-ranged" function of z, and this anisotropy of $S(\boldsymbol{r})S^\dagger(\boldsymbol{r}')$ leads to the angular anisotropy of $W(\boldsymbol{p}_m)$ shown in Figs. 1,2. One of the striking effects in Fig. 1,2 is the forward-backward asymmetry $W(p_\perp, -p_z) \neq W(p_\perp, p_z)$, which has its origin in the the nonvanishing real part of the p-n scattering amplitude $\rho \neq 0$, leading to $S(b, z)S^\dagger(b', z') \neq S(b', z')S^\dagger(b, z)$ in the integrand of (1). At small $p_m \ll 1$ fm^{-1} the angular distribution is isotropic, with increasing p_m it first develops an approximately symmetric dip at $\theta = 90°$. Fig. 2 shows how this dip evolves, through the very asymmetric stage, into the approximately symmetric peak at 90° at larger values of p_m. Fig. 1d shows the PWIA-FSI decomposition of the same 90° distribution. Shown by the dotted curve is the PWIA distribution, the dashed curve shows the pure rescattering contribution $\propto \Gamma^*\Gamma$ in Eq. (1). The term $\propto (\Gamma + \Gamma^*)$ from interference of the FSI and PWIA amplitudes, not shown separately here, is given by the difference between the solid curve and the sum of the dashed and dotted curves and is most significant around $p_m \sim 1.5$ fm^{-1}. The sharp peak at $\theta = 90°$, which emerges at $p_m \gtrsim 1.7$ fm^{-1}, is a pure
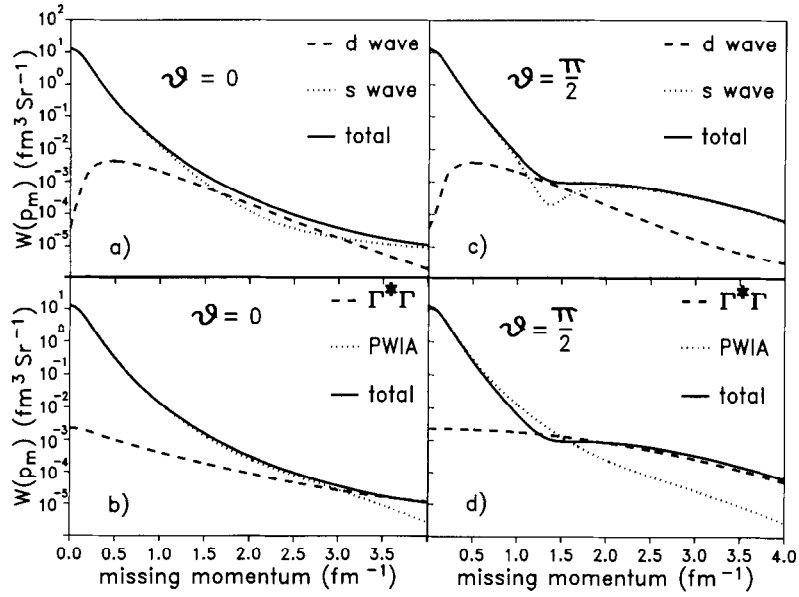
Fig. 1. The missing momentum distribution $W(p_m)$ vs. p_m and its decomposition into (a,c) the S and D-wave contributions and (b,d) into the PWIA and the rescattering contributions $\propto \Gamma^* \Gamma$ at (a,b) $\theta = 0°$ and (c,d) $\theta = 90°$. In panels (b,d) the full distribution $W(p_m)$ (the solid curve) includes also the contribution $\propto (\Gamma^* + \Gamma)$ from the interference of the PWIA and FSI amplitudes, which is not shown separately.
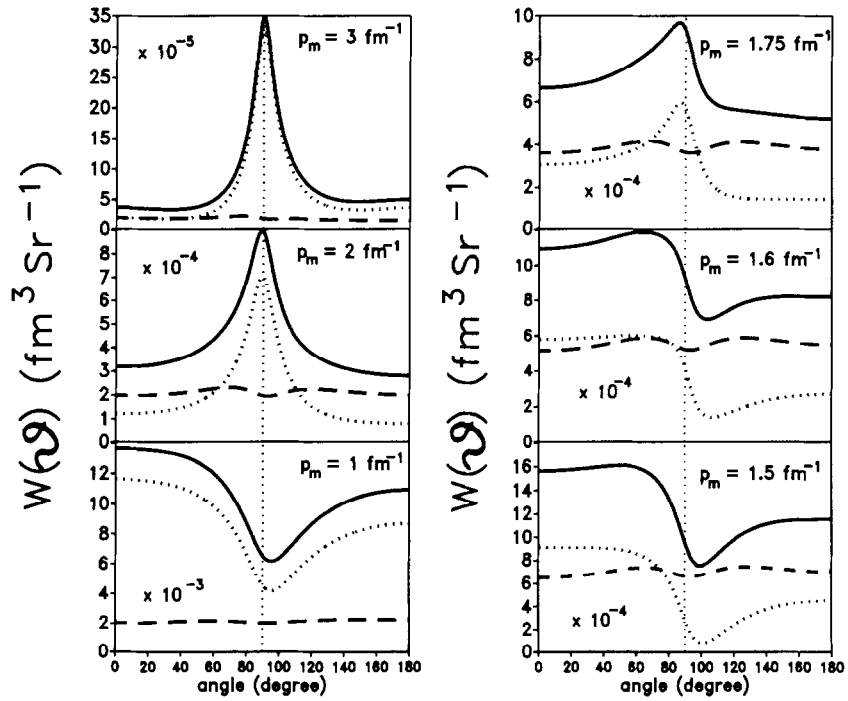

Fig. 2. The angular dependence of (solid curve) the missing momentum distribution $W(p_m)$ and of its (dotted curve) S-wave and (dashed curve) D-wave components at different values of the missing momentum p_m.

FSI (elastic *p-n* rescattering) effect.

It is well known ([8] and references therein) that in the PWIA, the large-p_m tail of the momentum distribution $n(p_m)$ is dominated by the D-wave contribution. The fact that $\Gamma(b)$ is a "short-ranged" function, whereas the D-wave function $w(r)$ is strongly suppressed at small distances by the centrifugal barrier, implies that FSI effects in the D-wave contribution to $W(p_m)$ should be much weaker than in the S-wave contribution. Indeed, Fig. 2 shows that although the D-wave contribution to $W(p_m)$ develops a nontrivial angular dependence, the overall departure from the isotropic PWIA distribution is rather small. Fig. 1(a,b) shows that the D-wave contribution remains a dominant component of $W(p_m)$ in parallel kinematics, but not in transverse kinematics, see Fig. 1(c,d).

The angular asymmetry mostly comes from the S-wave contribution which can conveniently be written as $W_S(p_m) = 2^{-5}\pi^{-4}U^2(p_m)$, where

$$U(p_m) = \int d^3r \exp(-ip_m \cdot r)S(r)\frac{u(r)}{r}$$
$$= u(1; p_m) - u(\Gamma; p_m). \quad (4)$$

The PWIA term $u(1; p_m)$ in (4) decreases on the scale $p_\perp, p_z \sim 1/R_D$. In view of $b_0^2 \ll R_D^2$, the FSI term $u(\Gamma; p_m)$ has the $p_\perp$ dependence $\sim \exp(-\frac{1}{2}b_0^2p_\perp^2)$ and at moderately large p_z it decreases on the scale $p_z \sim 1/R_D$ [3,4]. It has the small absolute normalization $\sim \sigma_{tot}(pn)/(2\pi R_D^2)$ [3,4]. The destructive interference of the PWIA and FSI amplitudes produces a dip in the S-wave contribution at $p_\perp \sim 1.3\,\text{fm}^{-1}$ as shown in Fig. 1c, which is partly filled by the effect of the finite ρ.

Fig. 1b shows that for $p_m \gtrsim 1.5\,\text{fm}^{-1}$, FSI effects are substantial also in parallel kinematics. Here the most interesting effect first noticed in [3], is the emergence of forward and backward peaks in $W(p_m)$ with increasing p_m as shown in Fig. 3. In Fig. 1b, the same effect shows up as the FSI component overwhelming the PWIA component at $p_m \gtrsim 3\,\text{fm}^{-1}$. The origin of this phenomenon is in the high-frequency Fourier components of the step-function $\theta(z)$ in the integrands of (1,4). The dominant effect comes from the "elastic rescattering" operator $\theta(z)\theta(z')\Gamma(b)\Gamma^*(b')$ in the integrand of (1), and Fig. 1b shows that the excess over the PWIA curve at $p_m \gtrsim 3\,\text{fm}^{-1}$ is entirely
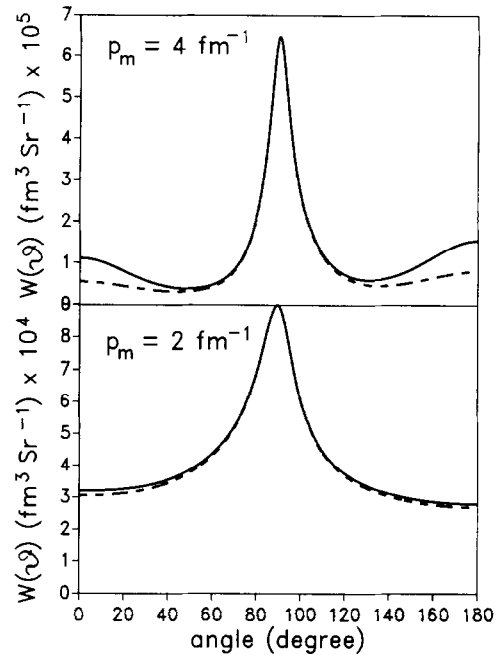

Fig. 3. The angular dependence of (solid curve) the missing momentum distribution $W(p_m)$ showing the development of the forward and backward peaks at large p_m. The dashed curve shows $W(p_m)$ found with the smeared step-function $T(z)$ of Eq. (5) with $z_0 = 0.25\,\text{fm}$.

due to the contribution from the term $\propto \Gamma^*\Gamma$. The scale for the intranucleon separation at which nucleons can still be treated as approximately structureless particles interacting with the free-nucleon amplitude, is set by the radius of the nucleon and/or the short-range correlation radius $r_c \sim 0.5\,\text{fm}$. The effect of the non-pointlike nucleons can be modelled substituting the idealized step-function $\theta(z)$ for the smeared one

$$T(z) \equiv \frac{1}{2}[1 + \tanh(\frac{z}{z_0})]. \quad (5)$$

The educated guess is $z_0 \lesssim \frac{1}{2}r_c$. In Fig. 3 we show the effect of smearing for $z_0 = \frac{1}{2}r_c = 0.25\,\text{fm}$. Uncertainties with the smearing do evidently persist at high Q^2. They are small at least up to $p_m \lesssim 3\,\text{fm}^{-1}$, treatment of higher p_m requires new approaches which go beyond the Glauber model.

The FSI-induced forward-backward asymmetry in parallel kinematics

$$A_{FB} = \frac{W(\theta = 0°, p_m) - W(\theta = 180°, p_m)}{W(\theta = 0°, p_m) + W(\theta = 180°, p_m)}$$
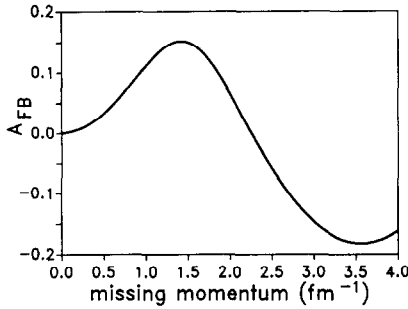
Fig. 4. The p_m dependence of the forward-backward asymmetry A_{FB} in parallel kinematics.

is shown in Fig. 4. The asymmetry A_{FB} is large and should be taken into account when looking for the forward-backward asymmetry which is expected at higher Q^2 because of the colour transparency effect [18] (see also a discussion in [6]).

Still another interesting quantity is the $p_\perp$-integrated, longitudinal missing momentum distribution $F(p_z) \equiv \int d^2 p_\perp W(p_\perp, p_z)$. In the PWIA, $F_{PWIA}(p_z) = \int d^2 p_\perp n(p_\perp, y)$ is related to the asymptotic y-scaling function [10]. In Fig. 5 we show the ratio $R(p_z) = F(p_z)/F_{PWIA}(p_z)$. At small p_z, the reduction of the flux of protons for the absorption by the neutron leads to a depletion $\sim 7\%$ in agreement with the estimate [4] and the NE18 experimental finding [19]. At larger $p_z \gtrsim 1.2\,\mathrm{fm}^{-1}$, the contribution $\propto \Gamma\Gamma^*$ from FSI enhances $F(p_z)$ by $\sim(30\text{--}40)\%$ as compared to the PWIA distribution $F_{PWIA}(p_z)$. At large $Q^2 \gtrsim 2\,\mathrm{GeV}^2$ and $T_{kin} = Q^2/2m_p \gtrsim 1\,\mathrm{GeV}$, the proton-neutron total cross section is approximately constant [17]. Therefore, this large FSI effect in $F(p_z)$ should persist at large $Q^2 \gg 1\,\mathrm{GeV}^2$ and should be taken into account in the asymptotic y-scaling regime, too. The departure from the PWIA further increases at $p_z \gtrsim 3\,\mathrm{fm}^{-1}$, but the quantitative description of FSI in this region of p_m requires improving upon the Glauber approach, which goes beyond the scope of this paper.

To summarize the main points, in this analysis of $D(e, e'p)$ scattering in the few-GeV region we have found that FSI effects completely dominate the observed missing momentum distribution $W(p_m)$ at high p_m (over $\sim 1.5\,\mathrm{fm}^{-1}$). They produce a marked angular anisotropy in $W(p_m)$, consisting in a dip at $\theta \sim 90°$ (in transverse kinematics) for $p_m \sim(1\text{--}1.5)\,\mathrm{fm}^{-1}$, and a prominent peak at the same angle for larger
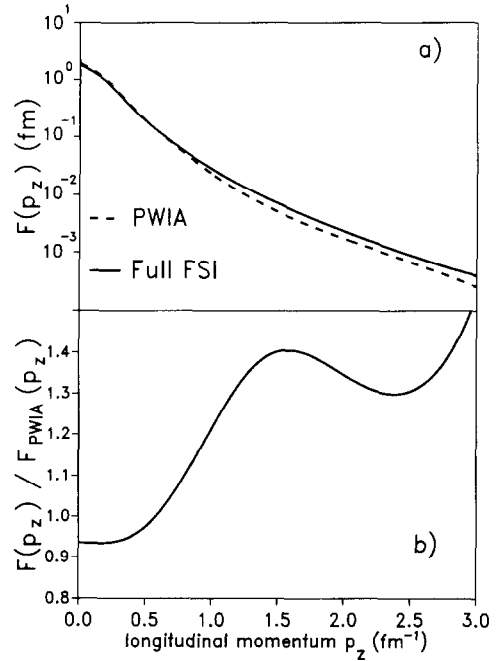

Fig. 5. (a) The longitudinal missing momentum distribution $F(p_z)$ calculated with full FSI (solid curve) and in the PWIA (dashed curve). (b) The ratio of the full $F(p_z)$ to the PWIA distribution $F_{PWIA}(p_z)$.

p_m. This anisotropy is mostly due to the FSI distortions of the S-wave contribution. The anisotropy effects in the D-wave contribution are also sizable, but much smaller than in the S-wave contribution. The D-wave contribution remains the dominant component for $p_m \gtrsim 1.5\,\mathrm{fm}^{-1}$ in parallel kinematics. The forward and backward peaks in the angular distribution at large $p_m \gtrsim 3\,\mathrm{fm}^{-1}$ are sensitive to modifications of the idealized θ-function in the FSI operator (2). As far as the applicability of Glauber's multiple scattering theory is concerned, this is an entirely new situation and shows that the Glauber treatment of FSI in $A(e, e'p)$ scattering is not fully self-contained at large longitudinal missing momenta. Glauber theory description of the proton-nucleus elastic scattering is very accurate [13–15], but in the pA scattering one has the well defined asymptotic $|in\rangle$ and $|out\rangle$ proton states, whereas in FSI in the $D(e, e'p)$ scattering the incoming proton wave is generated at a finite distance from the target neutron. When this distance becomes of the order of the radius of nucleons, one can not describe the distortion of the wave function of the spectator neutron by formula (2) with the idealized step-function.

We found large, $\sim 40\%$, FSI corrections to the longitudinal missing momentum distribution. FSI in the $D(e, e'p)$ scattering was discussed also in the recent work [20] using a different technique. These authors focused on corrections to the y-scaling analysis and did not consider the angular anisotropy of FSI effects. The numerical estimates of [20] for the FSI corrections to the longitudinal missing momentum distribution are close to ours.

We considered the charge operator relevant to the longitudinal response, but evidently our main conclusions on large FSI effects are also applicable to the transverse response. We focused on the dominant spin-independent FSI effects. The longitudinal cross section difference $\Delta\sigma_L(pn)$ has an interesting energy dependence around $T_{kin} \sim 1$ GeV, but is small, $\lesssim (10–20)\%$ of $\sigma_{tot}(pn)$ [17], and shall lead to an equally small, energy-dependent, correction to the predicted FSI effects. Also, besides the real part of the pn scattering amplitude, the spin-orbit interaction, too, shall partly fill in the dip at $p_m \sim 1.5\,\text{fm}^{-1}$ in transverse kinematics. The FSI effects in polarization observables and difference between FSI effects in transverse and longitudinal response will be discussed elsewhere.

References

[1] K. Gottfried, Ann. Phys. (USA) 21 (1963) 29;
W. Czyz and K. Gottfried, Nucl. Phys. 21 (1961) 676;
Ann. Phys. (USA) 21 (1963) 47.

[2] A.E.I. Dieperink and P.K.A. de Witt Huberts, Annu. Rev. Nucl. Part. Sci. 40 (1990) 239;

S. Boffi, C. Giusti and F.D. Pacati, Phys. Rep. 226 (1993) 1.

[3] A. Bianconi, S. Jeschonnek, N.N. Nikolaev and B.G. Zakharov, Jülich preprint KFA-IKP(Th)-1994-29 (1994), to appear in Phys. Lett. B.

[4] N.N. Nikolaev, A. Szczurek, J. Speth, J. Wambach, B.G. Zakharov and V.R. Zoller, Phys. Rev. C 50 (1994) R1296.

[5] N.N. Nikolaev, A. Szczurek, J. Speth, J. Wambach, B.G. Zakharov and V.R. Zoller, to appear in Nucl. Phys. A.

[6] J. Nemchik, N.N. Nikolaev and B.G. Zakharov, Color transparency after the NE18 and E665 experiments: Outlook and perspectives at CEBAF, Jülich preprint KFA-IKP(Th)-1994-20 (1994), to be published in Proceedings of the Workshop on CEBAF at Higher Energies, 14–16 April 1994.

[7] J. Mougey (spokesperson), CEBAF Proposal No. E-89-044;
R.G. Milner (spokesperson), CEBAF Proposal No. E-91-007;
D.F. Geesaman (spokesperson), CEBAF Proposal No. E-91-011.

[8] C. Marchand et al., Phys. Rev. Lett. 60 (1988) 1703.

[9] R. Machleidt, K. Holinde and C. Elster, Phys. Rep. 149 (1987) 1.

[10] G.B. West, Phys. Rep. 18 (1975) 264;
C. Ciofi degli Atti, E. Pace and G. Salme, Phys. Rev. C 43 (1991) 1155, and references therein.

[11] R.J. Glauber, in: Lectures in Theoretical Physics, v. 1, ed. W. Brittain and L.G. Dunham, Interscience Publ., N.Y., 1959;
R.J. Glauber and G. Matthiae, Nucl. Phys. B 21 (1970) 135.

[12] W. Fabian and H. Arenhövel, Nucl. Phys. A 445 (1976) 461;
H. Arenhövel and M. Sanzone, Few Body Systems, Supplementum 3 (1991).

[13] M. Bleszynski et al., Phys. Lett. B 87 (1979) 198.

[14] V. Braun, L.G. Dakhno and V.A. Nikonov, Sov. J. Nucl. Phys. 44 (1986) 848.

[15] G.D. Alkhazov, S.I. Belostotsky and A.A. Vorobyev, Phys. Rep. 42 (1978) 89.

[16] T. Lasinski et al., Nucl. Phys. B 37 (1972) 1.

[17] C. Lechanoine-LeLuc and F. Lehar, Rev. Mod. Phys. 65 (1993) 47.

[18] B. Jennings and B.Z. Kopeliovich, Phys. Rev. Lett. 70 (1993) 3384;
N.N. Nikolaev, A. Szczurek, J. Speth, J. Wambach, B.G. Zakharov, and V.R. Zoller, Phys. Lett. B 317 (1993) 287;
A. Bianconi, S. Boffi and D.E. Kharzeev, Phys. Lett. B 325 (1994) 294.

[19] T.G. O'Neill et al., submitted to Phys. Rev. Lett. (1994).

[20] C. Ciofi degli Atti and S. Simula, Phys. Lett. B 325 (1994) 276.